Electronic Supplementary Material (ESI) for Journal of Materials Chemistry A.
This journal is © The Royal Society of Chemistry 2023

Electronic Supplementary Information (ESI)

Tailoring Composite Polymer Electrolytes with Regularly Arranged Pores and Silica Particles for Sodium Metal Batteries via Breath-Figure Self-Assembly

Da-Sol Kwon,[ab] Daun Jeong,[a] Hyun Beom Kang,[ac] Wonyoung Chang,[a] Joona Bang[b] and Jimin Shim*[ad]

[a] Energy Storage Research Center, Korea Institute of Science and Technology (KIST), 14 Gil 5 Hwarang-ro, Seongbuk-gu, Seoul 02792, Republic of Korea

[b] Department of Chemical and Biological Engineering, Korea University, 145, Anam-ro, Seongbuk-gu, Seoul 02841, Republic of Korea

[c] Department of Materials Science and Engineering, Korea University, 145, Anam-ro, Seongbuk-gu, Seoul 02841, Republic of Korea

[d] Department of Chemistry Education, Seoul National University, 1, Gwanak-ro, Gwanak-gu, Seoul 08826, Republic of Korea

* E-mail: jiminshim@snu.ac.kr (J. Shim)

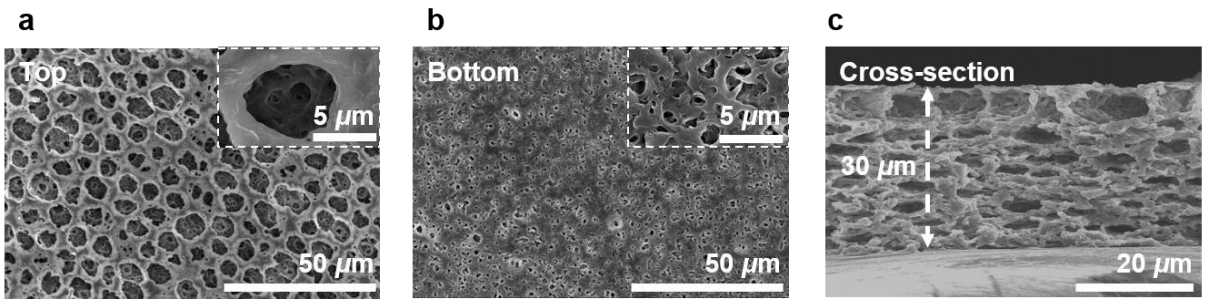

Fig. S1 (a) Top-surface, (b) bottom-surface, and (c) cross-sectional SEM images of PVH membrane prepared by static breath-figure self-assembly without silica particles.

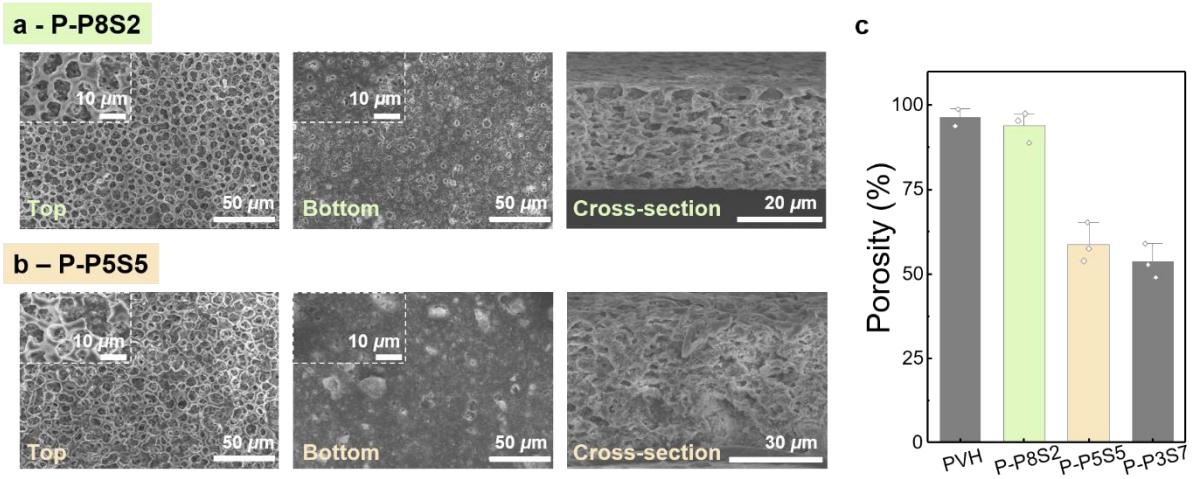

Fig. S2 SEM images of the (a) P-P8S2 and (b) P-P5S5 membranes. Note that the numbers next to P and S represent the weight fraction of PVH and silica particles, respectively. (c) Porosity (%) of the PVH, P-P8S2, P-P5S5, and P-P3S7.

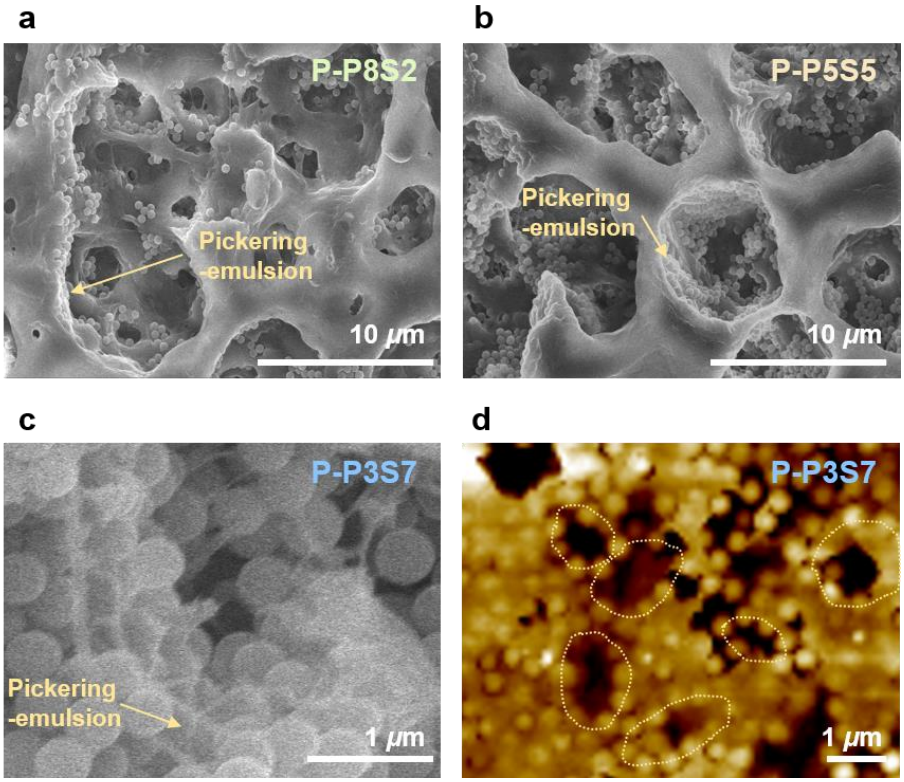

Fig. S3 SEM images of the (a) P-P8S2, (b) P-P5S5, and (c) P-P3S7 membranes, highlighting the Pickering-emulsion effect. (d) AFM image of the surface of P-P3S7.

As shown in Fig. S3a and b, both P-P8S2 and P-P5S5 show that silica particles are anchored onto the inner surfaces of the pores through the Pickering-emulsion effect. In contrast, the Pickering-emulsion effect was difficult to observe from P-P3S7, primarily due to its dense morphology with high-loading silica particles that fill the porous structure. However, as glimpsed in the SEM and AFM images in Figure S3c and d, it was found that silica particles are located along the pores of P-P3S7, indicating that the Pickering-emulsion effect is still effective in the P-P3S7.

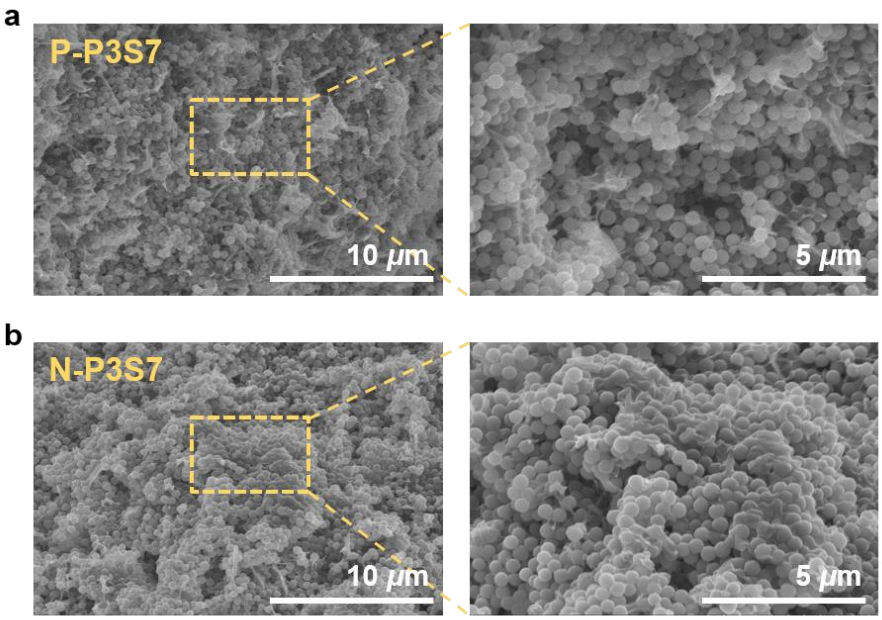

Fig. S4 Cross-sectional SEM images illustrating the dispersity of silica particles in the (b) P-P3S7 and (c) N-P3S7.

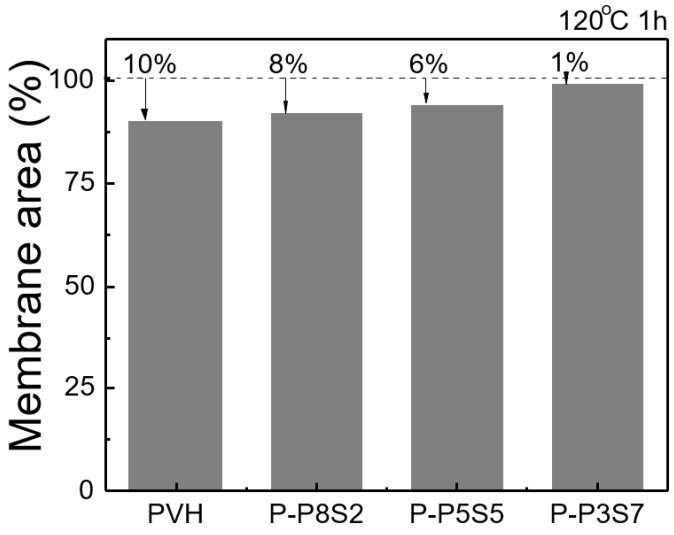

Fig. S5 Membrane area (%) after being exposed at 120 ℃ for 1 h.

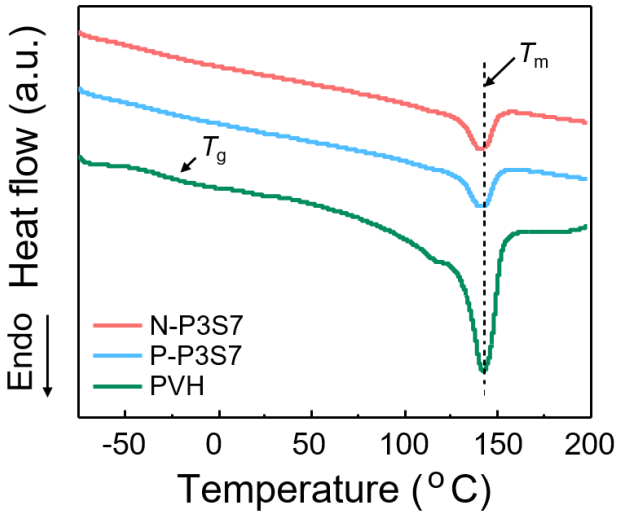

Fig. S6 DSC thermograms of PVH, P-P3S7, and N-P3S7.

As the silica particles are introduced to the PVH host, melting temperature (T_m) values of both P-P3S7 and N-P3S7 are slightly decreased, while the crystallinity is significantly decreased. This is primarily because silica particles disrupt the crystalline packing of PVH.[1] Additionally, it was observed that the glass transition temperature (T_g) value of the neat PVH is nearly absent in both P-P3S7 and N-P3S7. This is likely due to the incorporation of silica particles up to 70 wt%, which renders the polymer composite highly rigid, posing challenges in clearly identifying the T_g.

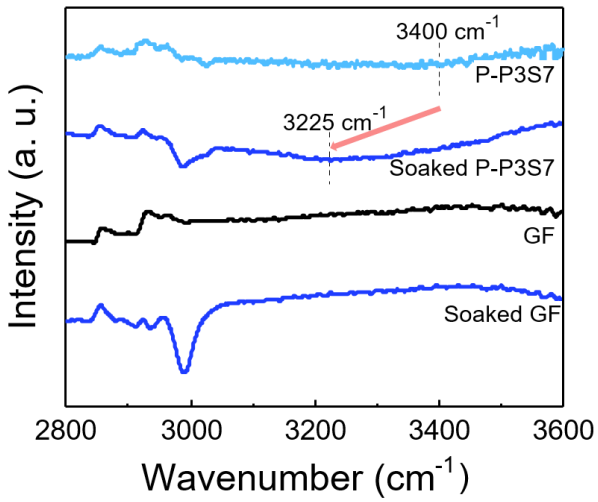

Fig. S7 FT-IR spectra of the GF and P-P3S7 before and after soaking in EC: PC: DEC (1:1:1 vol%) for 24 h.

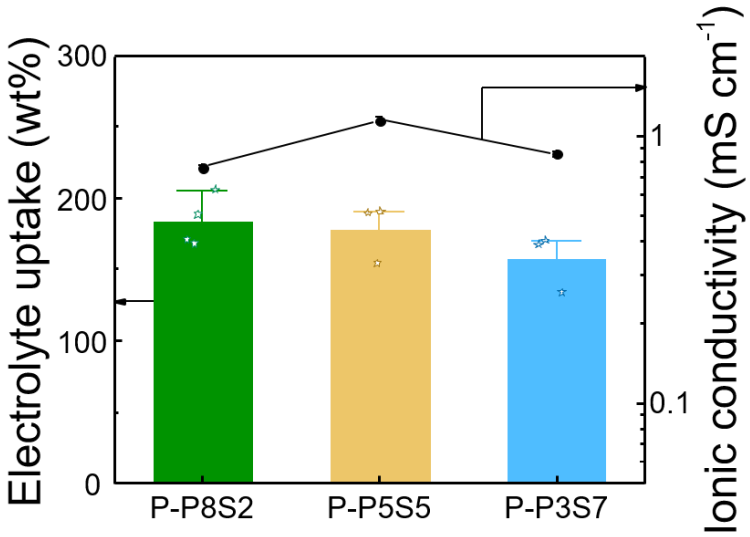

Fig. S8 Electrolyte uptakes and ionic conductivities of P-P8S2, P-P5S5, and P-P3S7 at room temperatures.

It was found that there are no significant differences between the electrolyte uptakes and ionic conductivities of the P-P8S2, P-P5S5, and P-P3S7. We speculate that the resulting electrolyte uptakes and ionic conductivities of the composite gel polymer electrolytes are not simply determined solely by their silica contents. As we described in section 2.3, the porosity, crystallinity of the PVH host, and Lewis acid-base interactions present in the system simultaneously affect the ion-conducting properties of the composite gel polymer electrolytes.

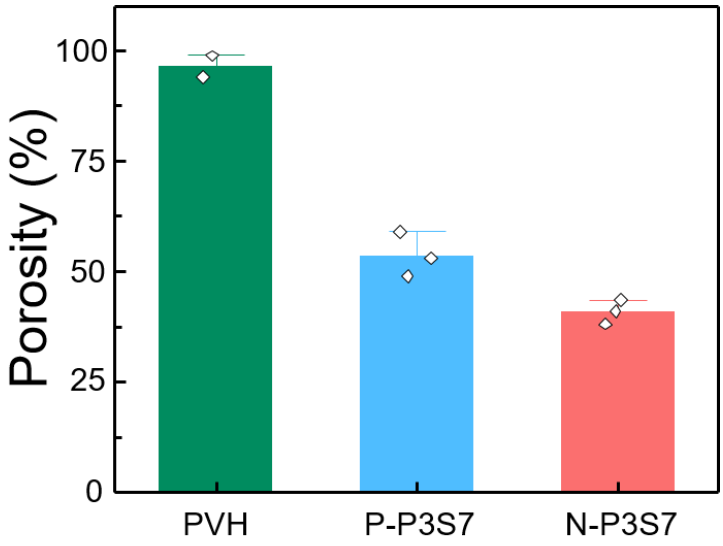

Fig. S9 Porosity values of the PVH, P-P3S7, and N-P3S7.

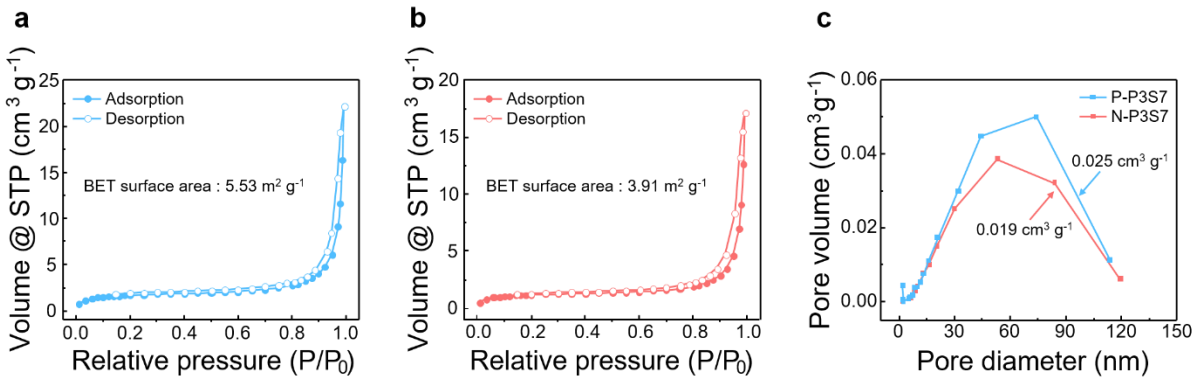

Fig. S10 BET analysis of P-P3S7 and N-P3S7. N_2 adsorption–desorption isotherms of (a) P-P3S7 and (b) N-P3S7, and the (c) corresponding BJH pore size distribution curve for P-P3S7 and N-P3S7.

As shown in Fig S10a and b, BET surface area values of 5.53 and 3.91 $m^2 g^{-1}$ were obtained for P-P3S7 and N-P3S7, respectively. The pore volume and average pore size were estimated by the BJH method as shown in Fig S10c. The pore volume and the average pore diameter of the P-P3S7 are 0.025 $cm^3 g^{-1}$ and 74 nm, respectively, and those of the N-P3S7 are 0.019 $cm^3 g^{-1}$ and 53 nm, respectively.

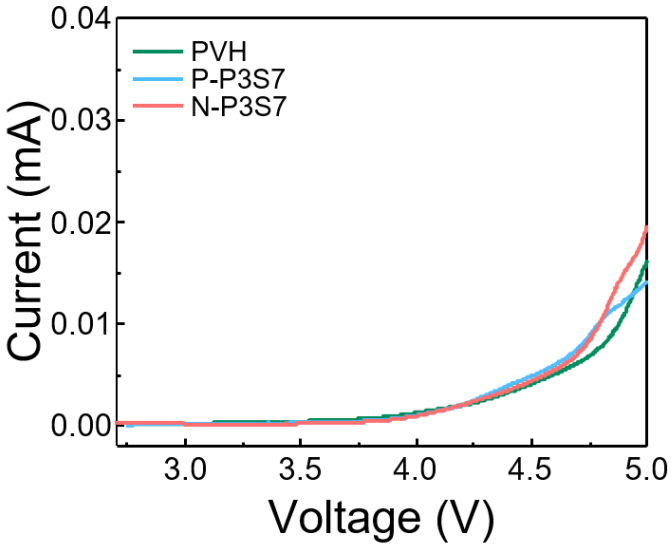

Fig. S11 LSV profiles of PVH, P-P3S7, and N-P3S7 (scan rate: 1 mV s^{-1}).

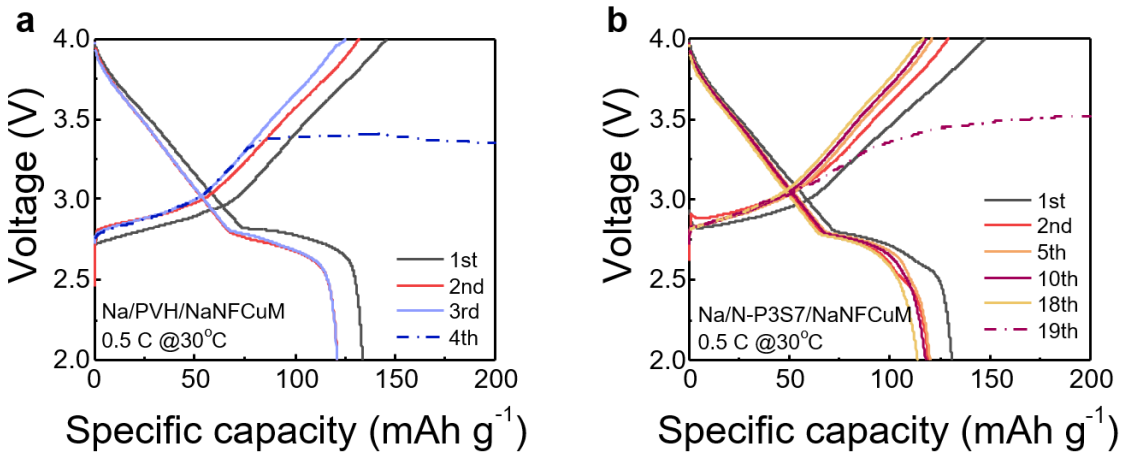

Fig. S12 Specific capacity-voltage profiles of the Na/NaNFCuM cells assembled with (a) PVH and (b) N-P3S7 cycled under 0.5 C at 30 ℃.

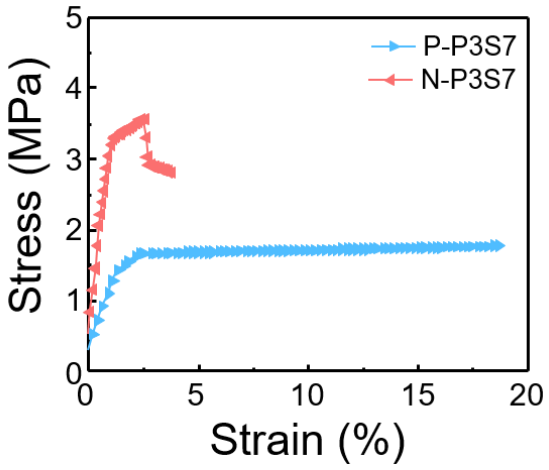

Fig. S13 Stress-strain curves of P-P3S7 and N-P3S7.

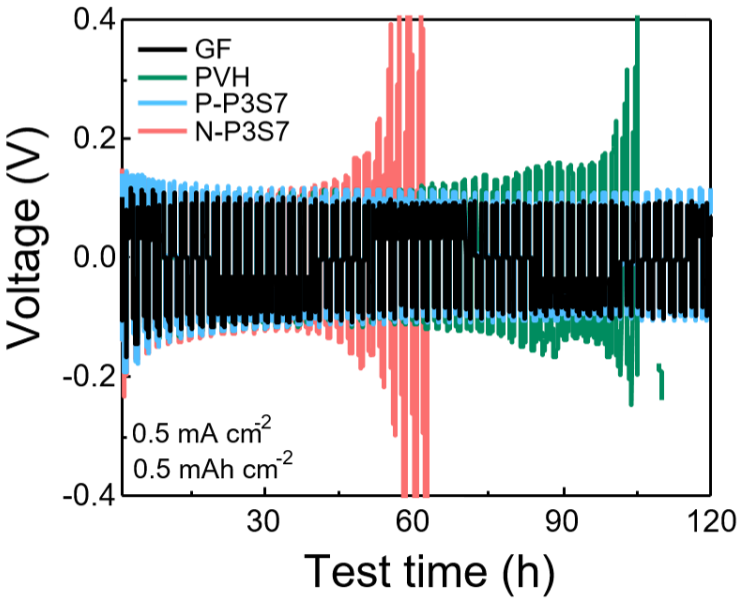

Fig. S14 Galvanostatic cycling profiles of symmetric Na/Na cells with GF, PVH, P-P3S7, and N-P3S7 at a current density of 0.5 mA cm^{-2} and a total capacity of 0.5 mAh cm^{-2} at 30 °C.

Both the GF and P-P3S7 cells show relatively stable overpotentials, while PVH and N-P3S7 cell exhibits an abrupt voltage increase after 90 h and 50 h, respectively. This finding is quite consistent with the cycling performance of Na/NaNFCuM cells in that only the GF and P-P3S7 cells were able to be cycled for 200 cycles, whereas the PVH and N-P3S7 cells showed abrupt cell failure accompanied by overcharging. This result further illustrates that the premature cell failure of PVH and P-P3S7 is primarily ascribed to Na dendrite growth.

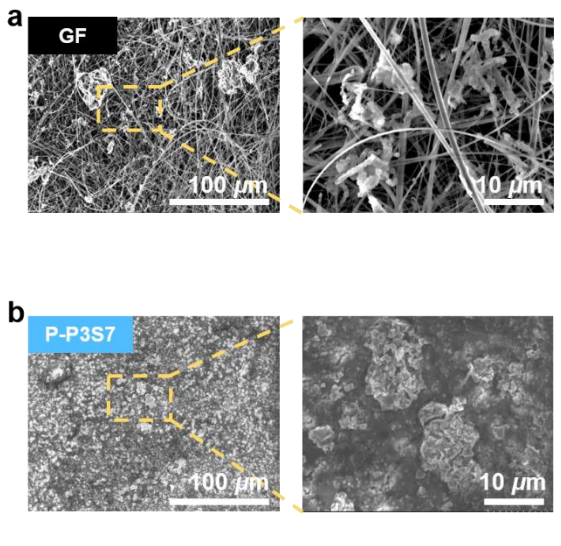

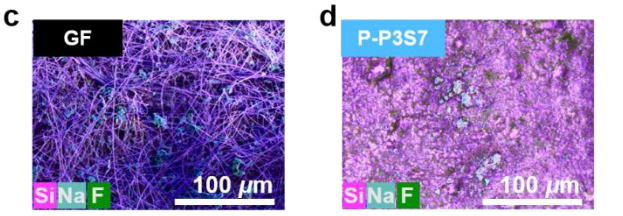

Element	Wt%	Atomic %
C	8.69	13.55
O	42.85	50.17
F	6.54	6.45
Na	13.21	10.76
Si	27.28	18.20
P	1.43	0.86
Total:	100.00	100.00

Element	Wt%	Atomic %
C	23.18	33.13
O	27.10	29.09
F	24.98	22.57
Na	0.70	0.52
Si	23.87	14.59
P	0.17	0.09
Total:	100.00	100.00

Fig. S15 SEM and EDS mapping images of the cathodic side of the (a,c) GF and (b,d) P-P3S7 membrane after 200 cycles.

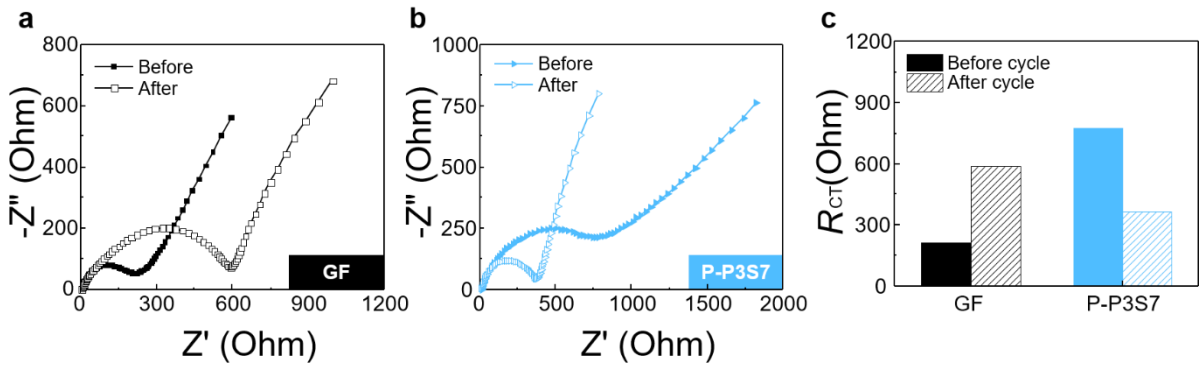

Fig. S16 EIS profiles of the Na/NaNFCuM cells assembled with (a) GF and (b) P-P3S7 cycled under 0.5 C at 30 ℃. (c) Summary of charge transfer resistances (R_{CT}) of the cells.

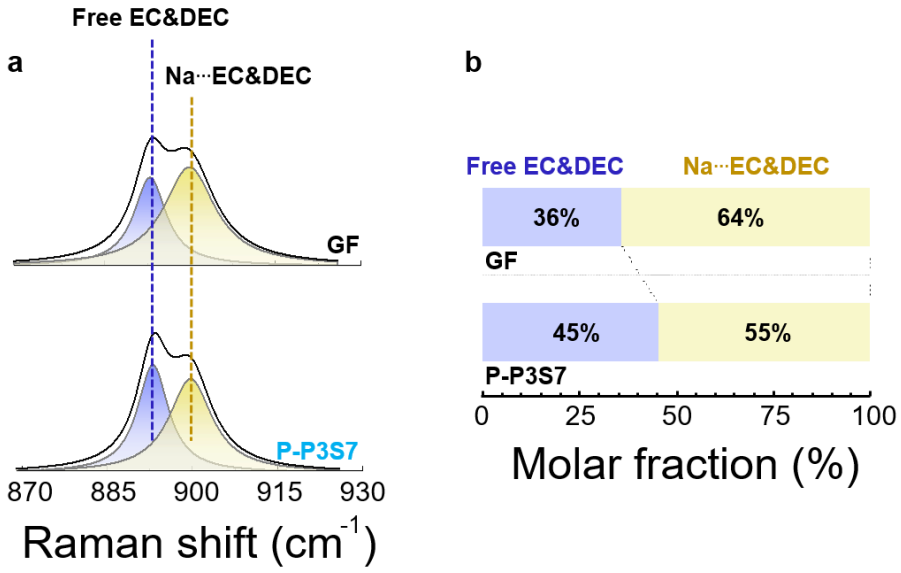

Fig. S17 (a) Deconvoluted Raman spectra of electrolyte-wetted GF and P-P3S7. (b) The summarized molar fraction of free and Na^+-coordinated C=O moieties in EC/DEC. Note that the membranes were immersed in 1 M $NaPF_6$ in EC: PC: DEC (1:1:1 vol%) with 2 wt% FEC for 24 h prior to the measurements.

The Na^+-coordination behavior was confirmed by Raman spectroscopy with the peaks at 893 and 900 cm^{-1} associated with free EC/DEC and Na^+-coordinated EC/DEC, respectively.[2]

Reference for Supporting Information

1 V. Aravindan and P. Vickraman, *J. Appl. Polym. Sci.* 2008, **108**, 1314-1322.
2 Z. Tang, H. Wang, P. F. Wu, S. Y. Zhou, Y. C. Huang, R. Zhang, D. Sun, Y. G. Tang and H. Y. Wang, *Angew. Chem. Int. Ed. Engl.* 2022, **61**, e202200475.